In silico karyotyping of chromosomally polymorphic malaria mosquitoes in the *Anopheles gambiae* complex

R. Rebecca Love[*], Seth N. Redmond[†1], Marco Pombi[‡], Beniamino Caputo[‡], Vincenzo Petrarca[‡], Alessandra della Torre[‡], The *Anopheles gambiae* 1000 Genomes Consortium[§], Nora J. Besansky[*††]

*Eck Institute for Global Health & Department of Biological Sciences, University of Notre Dame, Notre Dame, IN 46556, USA

[†]Infectious Disease and Microbiome Program, Broad Institute, Cambridge, MA 02142, USA

[‡]Dipartimento di Sanità Pubblica e Malattie Infettive, Istituto Pasteur Italia-Fondazione Cenci-Bolognetti, Università di Roma "La Sapienza", Piazzale Aldo Moro, 5, 00185 Rome, Italy

[§]https://www.malariagen.net/projects/ag1000g#people

[††]Corresponding author

[1]Present address: Monash University, Institute of Vector-Borne Disease, 3800, Clayton, Australia

22 **Running Title:** In silico karyotyping in malaria mosquitoes

23

24 **Key Words:** *Anopheles gambiae*, chromosomal inversion polymorphism, genomics,

25 inversion genotyping, karyotype analysis, malaria vector, tag SNP

26

27 **Corresponding Author:** Nora J. Besansky, Department of Biological Sciences,

28 University of Notre Dame, Notre Dame, IN 46556 USA, nbesansk@nd.edu

Abstract

Chromosomal inversion polymorphisms play an important role in adaptation to environmental heterogeneities. For mosquito species in the *Anopheles gambiae* complex that are significant vectors of human malaria, paracentric inversion polymorphisms are abundant and are associated with ecologically and epidemiologically important phenotypes. Improved understanding of these traits relies on determining mosquito karyotype, which currently depends upon laborious cytogenetic methods whose application is limited both by the requirement for specialized expertise and for properly preserved adult females at specific gonotrophic stages. To overcome this limitation, we developed sets of tag SNPs inside inversions whose biallelic genotype is strongly correlated with inversion genotype. We leveraged 1,347 fully sequenced *An. gambiae* and *Anopheles coluzzii* genomes in the Ag1000G database of natural variation. Beginning with principal components analysis (PCA) of population samples, applied to windows of the genome containing individual chromosomal rearrangements, we classified samples into three inversion genotypes, distinguishing homozygous inverted and homozygous uninverted groups by inclusion of the small subset of specimens in Ag1000G that are associated with cytogenetic metadata. We then assessed the correlation between candidate tag SNP genotypes and PCA-based inversion genotypes in our training sets, selecting those candidates with >80% agreement. Our initial tests both in held-back validation samples from Ag1000G and in data independent of Ag1000G suggest that when used for *in silico* inversion genotyping of sequenced mosquitoes, these tags perform better than traditional cytogenetics, even

51 for specimens where only a small subset of the tag SNPs can be successfully

52 ascertained.

Introduction

A chromosomal inversion originates when a chromosome segment reverses end to end. Inversions maintained in plant and animal populations as structural polymorphisms tend to be large (several megabases) and contain hundreds of genes (reviewed in Wellenreuther and Bernatchez 2018). Long-term balancing selection can maintain these polymorphisms through millions of generations and multiple species radiations (Wellenreuther and Bernatchez 2018). Because recombination is greatly reduced between opposite orientations in inversion heterozygotes, inversions preserve selectively advantageous combinations of alleles despite homogenizing gene flow in collinear regions. Theory and mounting evidence implicate inversions in local adaptation, adaptive divergence, and range expansion, though the precise molecular mechanisms are rarely known (Hoffmann *et al.* 2004; Kirkpatrick and Barton 2006; Hoffmann and Rieseberg 2008; Schaeffer 2008; Kirkpatrick 2010; Lowry and Willis 2010; Joron *et al.* 2011; Jones *et al.* 2012; Kirkpatrick and Barrett 2015; Twyford and Friedman 2015; Kapun *et al.* 2016; Ayala *et al.* 2017; Fuller *et al.* 2017; Wellenreuther *et al.* 2017; Wellenreuther and Bernatchez 2018). Importantly, because of occasional double-crossovers and gene conversion, the suppression of gene flux is not absolute. As long as inversion heterozygotes are formed in populations, any significant association between an inversion and an allele within its boundaries is subject to eventual erosion unless gene flux is countered by selection (Navarro *et al.* 1997; Andolfatto *et al.* 2001).

The *Anopheles gambiae* complex is a medically important group of at least eight closely related and morphologically indistinguishable mosquito sibling species from sub-Saharan Africa (White *et al.* 2011; Coetzee *et al.* 2013). Three members of the complex (the eponymous *Anopheles gambiae*, *Anopheles coluzzii*, and *Anopheles arabiensis*) are among the most significant malaria vectors globally, responsible for a majority of the 435,000 malaria deaths in 2017 (World Health Organisation 2018). The ecological plasticity of these three species contributes greatly to their status as major human malaria vectors (Coluzzi *et al.* 2002). In contrast to the other five, these three species have wide distributions across diverse biomes of tropical Africa. Not coincidentally, they also segregate strikingly high numbers of paracentric inversion polymorphisms, which are implicated in adaptation to seasonal and spatial environmental heterogeneities related both to climatic variables and anthropogenic alterations of the landscape (Coluzzi *et al.* 1979; Bryan *et al.* 1982; Coluzzi *et al.* 1985; Toure *et al.* 1998; Manoukis *et al.* 2008; Costantini *et al.* 2009; Simard *et al.* 2009; Cheng *et al.* 2012; Ayala *et al.* 2014; Caputo *et al.* 2014; Ayala *et al.* 2017; Cheng *et al.* 2018). Some of these inversions also have been associated with ecologically relevant phenotypes, including desiccation and thermal tolerance (Gray *et al.* 2009; Rocca *et al.* 2009; Cassone *et al.* 2011; Fouet *et al.* 2012; Ayala *et al.* 2018; Cheng *et al.* 2018).

The sister taxa *An. gambiae* and *An. coluzzii*, the focus of the present investigation, are the most closely related species in the *An. gambiae* complex, sharing extensive nucleotide variation through both recent common ancestry and introgression (Fontaine *et al.* 2015; Hanemaaijer *et al.* 2018), while maintaining characteristic differences in ecology and behavior (Costantini *et al.* 2009; Diabate *et al.* 2009; Simard

et al. 2009; Gimonneau *et al.* 2010; Gimonneau *et al.* 2012a; Gimonneau *et al.* 2012b; Dabire *et al.* 2013; Tene Fossog *et al.* 2015; Ayala *et al.* 2017). They also share four of six common chromosomal inversion polymorphisms on chromosomal arm 2R (*b*, *c*, *d*, *u*) and the only inversion polymorphism on chromosomal arm 2L (*a*) (Figure 1) (della Torre *et al.* 2005). These inversions range in size from ~4Mb to 22Mb, and together span thousands of genes and a sizeable fraction of chromosome 2: ~61% of 2R and ~38% of 2L polytene (euchromatic) content (Coluzzi *et al.* 2002). Inversions 2L*a* and 2R*b* are found in populations throughout tropical Africa and are therefore cosmopolitan, while three other inversions on 2R (*c*, *d*, and *u*) are widespread in West, very rare in Central Africa, and absent from East Africa. The remaining two inversions, 2R*j* and 2R*k*, have more restricted geographic distributions (Coluzzi *et al.* 2002; Ayala *et al.* 2017).

Early cytogenetic studies of *An. gambiae* and *An. coluzzii*, presumed at the time to be a single heterogenous species, uncovered genetic discontinuities that led to the designation of five presumed assortatively-mating 'chromosomal forms': FOREST, SAVANNA, MOPTI, BAMAKO, and BISSAU (Coluzzi *et al.* 1985; Toure *et al.* 1998; Coluzzi *et al.* 2002; della Torre *et al.* 2005). They were delineated based on stable non-random associations of different sets of chromosome 2R inversions in co-occurring populations, and differed in larval ecology. Subsequent DNA-based studies identified fixed differences in the ribosomal DNA (rDNA), located in the pericentromeric region of the X chromosome, leading to the definition of two assortatively mating M and S 'molecular forms' of *An. gambiae* (della Torre *et al.* 2001). The molecular forms, which were eventually given specific status as *An. coluzzii* (formerly M) and *An. gambiae sensu stricto* (formerly S) (Coetzee *et al.* 2013), are incongruent with the chromosomal

121 forms. Nearly all inversion associations segregate in both species albeit at different
122 frequencies, and likely play similar roles in ecological specialization and adaptation in
123 both *An. gambiae s.s.* (hereafter, *An. gambiae*) and *An. coluzzii* (della Torre *et al.* 2005;
124 Costantini *et al.* 2009; Simard *et al.* 2009; Ayala *et al.* 2017). Hence, inversion
125 associations are indicative of environmental heterogeneities more so than intrinsic
126 reproductive boundaries.

127 Beyond a role in ecological specialization, inversions in the *An. gambiae* complex
128 are also associated with vector traits affecting malaria transmission intensity and
129 control: biting and resting behavior (Coluzzi *et al.* 1979; Riehle *et al.* 2017), seasonality
130 (Rishikesh *et al.* 1985), morphometric variation (Petrarca *et al.* 1990), and *Plasmodium*
131 infection rates (Petrarca and Beier 1992; Riehle *et al.* 2017). Although a robust
132 molecular assay is available for genotyping inversion 2L*a* in natural populations (White
133 *et al.* 2007), 2R inversions with characterized breakpoint sequences (*j*, *b*, *c*, and *u*)
134 (Coulibaly *et al.* 2007a; Sangare 2007; Lobo *et al.* 2010) proved difficult to genotype
135 molecularly at the breakpoints (Coulibaly *et al.* 2007b; Lobo *et al.* 2010), owing to
136 extensive tracts of flanking repetitive DNA. The 2R*k* breakpoints have yet to be
137 characterized, but recent localization of the 2R*d* breakpoints in the reference genome
138 assembly using proximity-ligation sequencing (Corbett-Detig *et al.* 2019) also revealed
139 high repeat content, suggesting that repetitive DNA at inversion breakpoints will pose a
140 significant challenge both for breakpoint characterization and for molecular genotyping
141 assays targeting breakpoint regions in these species.

142 Failure to account for the presence of inversions is a barrier to a more
143 comprehensive understanding of epidemiologically relevant mosquito behavior and

144 physiology. Inversion-blind analysis of population data can mislead population genetic
145 inference, and create spurious associations in genome-wide association studies (Seich
146 Al Basatena *et al.* 2013; Houle and Marquez 2015). Powerful genomic resources exist
147 for *An. gambiae*, including a high-quality reference genome assembly (Holt *et al.* 2002)
148 and a database of genomic variation (Ag1000G) based on deep genome re-sequencing
149 of thousands of mosquitoes from natural populations across Africa (Miles *et al.* 2017).
150 Unfortunately, inversion genotypes are not automatically revealed by genome re-
151 sequencing, as reads are mapped to their position in the reference genome assembly,
152 not their position in the re-sequenced mosquito genome. Despite advancing genome
153 technology, the only method currently available to determine the *An. gambiae* karyotype
154 is a method perfected half a century ago (Coluzzi 1968) involving cytological analysis of
155 ovarian nurse cell polytene chromosomes (Coluzzi *et al.* 2002; Pombi *et al.* 2008). At
156 best, such cytological analysis is severely rate-limiting because it is laborious and
157 requires highly specialized training. At worst, it is prohibitive because it requires proper
158 preservation of chromosomes harvested only from ovaries of adult females at a specific
159 gonotrophic stage; suitable polytenization is absent at other gonotrophic stages as well
160 as in males (della Torre 1997). While salivary glands of late fourth instar larvae also
161 contain chromosomes with an adequate degree of polytenization, and the banding
162 patterns of salivary and ovarian chromosomes are homologous in principle, most bands
163 are difficult to homologize due to a different pattern of chromosome 'puffing' (della Torre
164 1997), rendering this alternative impractical. To overcome these impediments, our goal
165 is to develop broadly accessible computational and molecular methods of genotyping
166 chromosomal inversions in individual specimens of *An. gambiae* and *An. coluzzii*.

Here, we exploit the Ag1000G database and leverage the subset of cytologically karyotyped specimens within that database to develop a computational approach for karyotyping applicable to whole genome sequence data. We identify multiple tag single nucleotide polymorphisms (SNPs) significantly associated with inversions across geography that collectively predict with high confidence the genotypes of six common polymorphic inversions on chromosome 2 (*a*, *j*, *b*, *c*, *d*, *u*) in individually sequenced genomes of *An. coluzzii* and *An. gambiae*. We then apply this approach to data generated independently of Ag1000G to show that our approach has wider utility, even for specimens where only a small subset of the tag SNPs can be successfully ascertained.

178

179 **Methods**

180

181 *Mosquito genotype data*

182 Variant call data used for the discovery of inversion tag SNPs were accessed from
183 Ag1000G (Miles *et al.* 2017) and Vector Observatory (VOBS; Table S1), projects of the
184 Malaria Genomic Epidemiology Network (MalariaGEN; https://www.malariagen.net/)
185 that provide catalogs of genomic sequence variation based on individual wild-collected
186 *An. gambiae* and *An. coluzzii* mosquitoes sampled from multiple African countries and
187 the Mayotte archipelago. With the exception of four atypical samples (see next section),
188 we verified species identifications as reported in Ag1000G and VOBS using principal
189 component analysis (PCA) of biallelic SNPs on the X chromosome. We excluded any
190 specimens with more than 50,000 missing genotypes on chromosomal arm 2R (N=9),
191 and any specimens subjected to whole genome amplification (WGA) prior to genomic
192 sequencing (N=44), as PCA revealed strong biases associated with WGA. After
193 filtering, we retained variant call data from 1,347 mosquitoes (Table S2).

194

195 *Karyotype imputation by local PCA*

196 Cytological karyotype information derived from phase contrast microscopy of ovarian
197 polytene chromosomes (della Torre 1997) was available only for a relatively small
198 subset of specimens (N=373) in Ag1000G/VOBS (hereafter, Ag1000G for brevity).
199 Thus, as a first step toward discovering SNPs putatively predictive of inversion status
200 (tag SNPs), we imputed karyotypes computationally at each of six focal inversions

(Figure 1), using local PCA (where 'local' refers to windows of the genome corresponding to chromosomal rearrangements). Ma and Amos (2012) showed that applying PCA to SNP genotypes in a window of the genome containing an inversion polymorphic in population genomic data (an approach that we call 'PCA karyotyping') produces a pattern of three equidistant clusters (stripes) in a plot of the first two principal components, assuming adequate numbers of each of three possible inversion genotypes: inverted and uninverted (standard) homokaryotypes, and heterokaryotypes. The two flanking stripes represent alternative homokaryotypes, and the middle stripe represents the inversion heterokaryotype, a 1:1 "admixture" between the two homokaryotype classes (Ma and Amos 2012).

To apply this approach, we combined specimens from both species (*An. gambiae* and *An. coluzzii*) and different geographic localities into a single metapopulation sample of 1,347 mosquitoes (Tables S1, S2). We identified a set of biallelic SNPs within inversion boundaries (Table S3) with potentially informative levels of polymorphism [minor allele count $\geq$3 and minimum alternate allele frequency (MAF) $\geq$0.15 for all inversions except 2R*d*, for which the MAF threshold was reduced to 0.03]. As 2R*d* overlaps 2R*u* in the genome (Figure 1), we limited consideration to only those SNPs found outside (proximal to) 2R*u* for PCA karyotyping of 2R*d* (Table S3). Next, we converted mosquito genotypes at these SNPs to a count of the number of alternate alleles ('0' if both matched the reference allele, '1' or '2' if one or both matched the alternate allele, respectively). Using the scikit-allel Python package v1.1.9 (Miles and Harding 2017), we then applied PCA to the resulting matrix of alternate allele counts, and represented the output as a scatter plot of the first two principal components for

each mosquito in the population sample. The correct genotype corresponding to the two homokaryotype stripes was determined based on the inclusion in a given stripe of mosquitoes with cytologically determined karyotype. Based on this classification, mosquitoes without cytologically determined karyotypes were assigned a PCA karyotype.

The distinction between stripes was not always sharp; the stripes could be diffuse and oblique rather than tightly clustered. In extreme cases, stripes were not initially discernable. Through an iterative process of 'leave one population sample out' followed by PCA, we determined that absence of a clear three-stripe pattern was attributable to some or all of the same four atypical source populations, in particular, those from Kenya, Mayotte, The Gambia, and Guinea Bissau. The Kenyan sample has been found to display signs of extreme inbreeding (Miles *et al.* 2017), and Mayotte is an island whose mosquito population is plausibly subject both to inbreeding and a degree of isolation from mainland samples. The Gambia and Guinea Bissau are localities with unusually high degrees of hybridization and introgression between *An. gambiae* and *An. coluzzii* (Caputo *et al.* 2008; Oliveira *et al.* 2008; Caputo *et al.* 2011; Marsden *et al.* 2011; Weetman *et al.* 2012; Nwakanma *et al.* 2013). Where necessary, we removed these population samples, as well as two *An. gambiae*-*An. coluzzii* hybrid specimens from Burkina Faso and Guinea Conakry, and repeated the PCA. In addition, successful PCA karyotyping of 2R*d* and 2R*j* required the removal of all *An. coluzzii* specimens owing to taxonomic structuring of variation. Accordingly, PCA karyotyping was successful on all (2L*a*) or subsets (all 2R inversions) of the 1,347 specimens (Table S4).

Discovery of SNPs predictive of inversion orientation

The PEST reference genome assembly for *An. gambiae* (AgamP4; Giraldo-Calderon *et al.* 2015) was derived from a colony whose karyotype was homozygous standard with respect to all common chromosomal inversions in this species. We therefore had the general expectation that an individual SNP might be a good predictor of chromosomal inversion orientation if the reference allele is strongly associated with the standard arrangement and the alternate allele is strongly associated with the inverted arrangement within and across population samples. As shown in Figure 2 in overview, we assessed SNP genotype-inversion genotype concordance for each inversion in individual mosquitoes, limiting our assessment to potentially more informative, higher frequency biallelic SNPs inside inversion boundaries (*i.e.*, those with MAF≥5%). We converted both the SNP genotype and the corresponding mosquito's PCA-based inversion genotype to single numbers, representing the count of alternate alleles (0, 1, or 2) in the case of SNP genotype, and the count of inverted chromosomes (0, 1, or 2) in the case of inversion genotype. Successfully performing tags are expected to have a SNP genotype that correlates strongly with the PCA-based inversion genotype.

More formally, we sought to identify candidate tag SNPs using the procedure illustrated in Figure 3 (applied separately for each inversion). Specimens assigned a PCA-based karyotype for a focal inversion were divided into a training sample used for tag SNP discovery (75%) and a validation sample that was held in reserve until a later time (25%), using the model_selection module of the scikit-learn Python package (v0.19.2) (Pedregosa *et al.* 2011). We ensured that both partitions were balanced with regard to inversion genotypes but randomized in all other respects. For robust

identification of candidate tag SNPs within the training sample, we masked all SNP genotypes inside the inversion boundaries with a genotype quality (GQ) below 20.

Next, we created ten bootstrap replicates of the training sample (Figure 3). Each of the ten replicates consisted of sub-samples of 75% of the full training sample, chosen at random with respect to all variables except inversion genotype balance. For each bootstrap replicate at each interrogated SNP (biallelic, MAF≥5%), we calculated the SNP genotype-inversion genotype concordance for each mosquito in the sample, as described above (Figure 2). Genotypic concordance at each SNP interrogated in a given bootstrap replicate was expressed as the percentage of mosquitoes for which the number of alternate SNP alleles matched the number of inverted chromosomes. Because an imbalance among inversion genotypes could lead to false-positive tag SNPs, we calculated concordance separately for the three inversion genotypes in each of the ten bootstrap replicates. We then averaged the concordance scores across the ten replicates, by inversion genotype. To generate a single, conservative tag SNP concordance statistic, we used the minimum of the three mean values. Note that because the mosquito composition differed among bootstrap replicates, some SNPs were not evaluated in all ten, if they did not pass our filters in one or more iterations. Finally, to eliminate SNP positions with high levels of missing genotypes, we also calculated for each inversion genotype in each bootstrap replicate the percentage of mosquitoes with SNP genotype calls at the candidate tag (the 'call rate'), and averaged across the ten replicates.

The procedure just described returned from 99 to 349 candidate tag SNPs for five inversions, but only two for 2R*c* (Table 1). We therefore adopted a modified

293 approach to control for suspected population structure. One possible source of
294 structure was the haplotype configuration of 2R*c* with respect to the flanking inversions
295 (2R*b* and 2R*u*) (Figure 1). The inverted orientation of 2R*c* is in almost perfect linkage
296 disequilibrium with the inverted orientation of either 2R*b* (as haplotype '2R*bc*') or 2R*u*
297 (as haplotype '2R*cu*'). In a ~50-year cytogenetic database compiled from samples
298 collected in many parts of sub-Saharan Africa (described in Pombi *et al.* 2008), only four
299 specimens were ever recorded as carrying the inverted orientation of 2R*c*
300 unaccompanied by either 2R*b* or 2R*u* (V. Petrarca, unpublished data). A second
301 source, not mutually exclusive, was population structure between *An. coluzzii*, *An.*
302 *gambiae*, and the BAMAKO chromosomal form that is subsumed taxonomically within
303 *An. gambiae* but is at least partially reproductively isolated and genetically differentiated
304 (Manoukis *et al.* 2008; Love *et al.* 2016). Although 2R*c* occurs in all three taxa, there is
305 a strong karyotype imbalance among them in natural populations and in Ag1000G. For
306 example, of 70 *An. coluzzii* with 2R*c* in Ag1000G, at least 49 (70%) carried the 2R*bc*
307 haplotype (haplotypes of the other specimens could not be inferred unambiguously).
308 Similarly, of 64 non-BAMAKO *An. gambiae* with 2R*c*, 62 (97%) carried the 2R*bc*
309 haplotype. On the other hand, all 45 BAMAKO, by definition, carried 2R*cu*. We initially
310 partitioned our sample by species, but the inclusion of BAMAKO in the *An. gambiae*
311 partition resulted in very few candidate tags concordant with inversion genotype (N=17).
312 Ultimately, we retained two data partitions (*An. coluzzii* and non-BAMAKO *An.*
313 *gambiae*), eliminating a third BAMAKO partition due to the fixation of 2R*c* in this taxon
314 (Coluzzi *et al.* 1985). From the non-BAMAKO *An. gambiae* partition (hereafter, *An.*
315 *gambiae* for brevity), we omitted two of only three specimens carrying 2R*u* (AZ0267-C

316 from Mali and AV0043 C from Guinea), guided by PCA. As described above, both data
317 partitions were split into training (75%) and validation (25%) sets, and ten bootstrap
318 replicates of each training set were analyzed.
319 Ultimately, the candidate tag SNPs chosen (Table 1) met the following three
320 criteria: they were (i) analyzed in at least eight of the ten bootstrap replicates; (ii) called
321 at a rate greater than 90% within each karyotype class; and (iii) concordant with
322 karyotype more than 80% of the time within each karyotype class (99.5% for 2L*a*).
323 Their approximate physical position relative to the span of each inversion is illustrated in
324 Figure S1.
325
326 *Validation of candidate tag SNPs in Ag1000G*
327 We interrogated the candidate tag SNPs in the validation samples from Ag1000G that
328 had been held aside during the discovery phase (Figure 3). For each mosquito in the
329 validation set, we masked genotypes inside the focal inversion with GQ scores less than
330 20. Next, among the retained SNPs, we identified those corresponding to candidate
331 tags and converted their diploid genotypes to a count of the number of alternate alleles.
332 Finally, the number of alternate alleles at each tag SNP was summed across tags and
333 averaged to provide an overall computational karyotype score. We compared this mean
334 score to the PCA-based karyotype.
335
336 *Testing tag SNPs in data independent of the Ag1000G pipeline*
337 We also explored the efficacy of our tag SNPs for computational karyotyping in wild-
338 caught mosquitoes subject to whole genome sequencing and variant calling by

individual investigators, for which corresponding cytological karyotypes had been determined through phase microscopy (Figure 3). We used specimens originating from southern Mali, 8 *An. gambiae* BAMAKO chromosomal form (Fontaine *et al.* 2015; Love *et al.* 2016) and 17 *An. coluzzii* (Main *et al.* 2015), whose variant calls and cytogenetic metadata are publicly accessible (Table S5). These data include specimens sequenced to much lower coverage than the standard adhered to by Ag1000G. We followed the same procedure described for the Ag1000G validation set to computationally karyotype these specimens, and compared their computational and cytologically determined karyotypes.

Genetic distance trees to assess inversion history

We compared patterns of relatedness near the breakpoints of all six inversions using unrooted neighbor-joining (NJ) trees. For each inversion, we used biallelic SNPs with a MAF of 0.01 found within 5 kb upstream and downstream of the distal and proximal breakpoints (15 kb for 2R*d*). Total numbers of SNPs for each inversion were: 2L*a*, 596; 2R*j*, 909; 2R*b*, 428; 2R*c*, 2141; 2R*d*, 955; 2R*u*, 1110. Using the python package *anhima*, we converted the number of alternate alleles at these SNPs into a Euclidean distance matrix, and then constructed neighbor-joining trees using all 1,347 specimens. To assess support for the nodes of the 2R*c* tree, we used the transfer bootstrap estimate (TBE; Lemoine *et al.* 2018), a statistic that measures the number of taxa that must be transferred to make a given branch of a reference tree match the closest equivalent branch in a bootstrap tree. To calculate this statistic, we imported the matrix of alternate allele counts into R (v. 3.5.1, “Feather Spray”; R Core Team 2018) and used

362 the dist() function of base R to construct the Euclidean distance matrix. We then used
363 the nj() function in the ape package (v. 5.2) to construct the neighbor joining tree, and
364 the boot.phylo() function to generate 1,000 bootstrap trees. We used these trees as
365 input to booster (Lemoine *et al.* 2018), which calculates the TBE for each node.
366
367 *Code and data availability*
368 All genomic sequence data and variant call files used in this study are located in open
369 data repositories as specified in Tables S1 and S2. The *An. gambiae* AgamP4
370 reference assembly is available through VectorBase (https://www.vectorbase.org/). All
371 custom code necessary to reproduce this analysis can be found at
372 https://github.com/rrlove/comp_karyo_notebooks and https://github.com/rrlove/ingenos.
373 The complete set of tag SNPs, together with a custom script for computational
374 karyotyping, which calculates the mean inversion genotype across the relevant tag
375 SNPs, can be found at https://github.com/rrlove/compkaryo.
376

Results

After filtering, we retained the genotype data from 1,347 individually sequenced *An. coluzzii* and *An. gambiae* mosquitoes from the Ag1000G repository of natural genomic sequence variation, representing population samples from 13 West, Central, and East African countries and the island of Mayotte (Tables S1, S2).

Patterns of genetic variation at inversion breakpoints

To gain insight into the relative roles of inversion history, taxonomic status, and geographic location in structuring genetic variation for each inversion, we reconstructed neighbor-joining trees based on SNPs in the immediate vicinity of the breakpoints (Figure 4). The resulting dendrograms, color-coded by inversion genotype, taxon and African country, indicate little clustering on the basis of geographic location; outlier population samples are those with a history of inbreeding or hybridization (see Methods). On the other hand, with the notable exception of 2L*a*, taxonomic status is an important factor structuring inversion variation between *An. gambiae* and *An. coluzzii*. Moreover, BAMAKO specimens appear to comprise a differentiated outlier clade within the larger *An. gambiae* cluster. It is interesting to note that for inversion 2R*c*, taxonomic status appears to be a more decisive factor than inversion genotype. All three 2R*c* inversion genotypes cluster within their respective species (supported by bootstrap at 90%, or 98% if dendrograms are constructed after removing outlier samples from The Gambia, Guinea-Bissau and Kenya; not shown). Further investigation is required to

399 determine whether this pattern results from a monophyletic inversion that subsequently
400 differentiated between taxa, or from independent inversion events in the two taxa.
401
402 *Inversion karyotype imputation by PCA*
403 Only 373 of the 1,347 mosquitoes were associated with metadata that included
404 cytologically determined inversion karyotypes. As discovery of candidate tag SNPs
405 requires provisional inversion genotype assignments, we applied local PCA to assign
406 genotypes for individual inversions on chromosome 2, following Ma and Amos (2012).
407 A recognized limitation to this population-level approach, beyond the fact that it cannot
408 be applied to individual mosquitoes, is that its success depends upon the presence of
409 all three inversion genotypes in the sample under study. For this reason, and with the
410 goal of finding the most flexible solution to inversion genotyping across geography and
411 taxa, we began with PCA based on the entire set of 1,347 mosquitoes, under the
412 simplifying assumption that the expected 'three-stripe' signal on a PCA plot would not
413 be overwhelmed by geographic or population structure. Only in the case of 2L*a* could
414 genotype assignments be confidently inferred from the combination of all 1,347
415 specimens. For inversions on 2R, from one to four admixed (*An. gambiae-An. coluzzii*)
416 or geographic outlier populations (highly inbred or island samples) had to be removed
417 from analysis before a three-genotype pattern could be discerned on the PCA plot
418 (Tables S2, S4; see Methods). Additionally, for 2R*d* and 2R*j*, *An. gambiae-An. coluzzii*
419 population structure dominated the PCA. Taken together with the fact that 2R*j* has yet
420 to be found in *An. coluzzii* (Coluzzi *et al.* 2002; della Torre *et al.* 2005), we removed all
421 341 *An. coluzzii* specimens (Tables S2, S4) prior to PCA karyotyping of 2R*d* and 2R*j* in

An. gambiae. Ultimately, PCA karyotypes were imputed for 780-1,347 mosquitoes, depending upon the inversion (Table S4).

Tag SNP ascertainment and validation in Ag1000G

Dividing the Ag1000G samples into training (75%) and validation (25%) sets for each inversion, and working within the training sets using a bootstrapping procedure, we screened for candidate tag SNPs in the five 2R inversions and 2L*a* (see Methods for details). Candidate tag SNPs were those whose genotypes were concordant with the corresponding PCA genotypes, when averaged across ten bootstrap replicates, for more than 80% of the specimens that were scored (99.5% for 2L*a*). The number of candidate tags ranged from 99 (2R*j*) to 349 (2R*b*) excluding 2R*c*, in which only two candidates were found due to population structure between *An. gambiae* and *An. coluzzii* (Figure 4; Table 1). Partitioning the 2R*c* sample by taxon (and omitting BAMAKO; see Methods) resulted in 49 and 57 tags for *An. gambiae* and *An. coluzzii*, respectively (Table 1). Notably, there was no overlap between the two sets of tags.

To assess the performance of these candidate tags, we used them to predict karyotypes in the held-out validation sets of Ag1000G specimens. For each inversion and specimen, we calculated a computational karyotype score representing the average genotype inferred across all candidate tag SNPs ascertained (see Methods). Histograms of resulting computational karyotype scores generally showed tight clustering around the three theoretical genotypic optima (0, 1, 2), reflecting close agreement among specimens (Figure 5). For each specimen in a validation set, we then compared the computational karyotype score to its PCA karyotype, and tallied the

number of disagreements (Table 2). All except one specimen had matching PCA and computational karyotype scores. This exception, one of 254 (0.4%) assignments for 2R*c* in *An. gambiae*, involved a specimen carrying 2R*u* (AZ0267-C) already noted as an outlier (see Methods).

Performance of tag SNPs in resequencing data independent of Ag1000G

Previous studies re-sequenced *An. gambiae* or *An. coluzzii* mosquitoes from Mali whose karyotypes had been determined from the polytene chromosome banding pattern (Main *et al.* 2015; Love *et al.* 2016). Although sample size is limited, these data allow a direct comparison of cytogenetic and *in silico* karyotyping under less ideal conditions—lower sequencing depth, with variant calls made independently of the Ag1000G pipeline. For each specimen and inversion, we calculated computational karyotype scores (averaged across all tag SNPs that could be ascertained in a specimen) (Tables S5, S6). Histograms of these scores by inversion, similar to those based on Ag1000G validation sets, reveal clustering of scores around the three genotypic optima provided that taxon-specific tags (2R*c-coluzzii* and 2R*c-gambiae*) are applied to the conspecific taxon, and heterospecific applications (including use of 2R*c-gambiae* tags to genotype BAMAKO) are avoided (Figure 6, Figure S2).

In the BAMAKO sample of Love *et al.* (2016) where mean sequencing depth ranged from 9-10x, there was concordance in karyotype assignments between cytogenetic and computational methods for five inversions including 2L*a*, even though only 10-12 2L*a* tags were ascertained (Table S5, S6). However, as expected for

BAMAKO, the *An. gambiae* 2R*c* tags failed. Due to the extreme geospatial restriction of BAMAKO, this specific problem is limited in scope.

In the *An. coluzzii* sample of Main *et al*. (2015), mean sequencing coverage varied widely (4-66x; Tables S5, S6). The impact of very low sequencing coverage on the success of computational karyotyping is illustrated by specimens 04SEL021 and 04SEL02 (4x and 5x, respectively). For 04SEL021, there is no apparent disagreement between the cytogenetic and mean computational genotype scores for any of the six inversions. Nevertheless, for those inversions classified as heterozygotes both cytogenetically and computationally (2L*a*, 2R*b*, 2R*c*), the proportion of tags whose genotype matches the mean computational score drops drastically to ~30% (Table S5), likely because true heterozygous sites are often scored as homozygous either for the reference or alternate allele (0 or 2) due to low sequencing coverage. (Indeed, using chromosome 3L, we confirmed the expected drop in the rate of heterozygosity with decreasing coverage in these 17 specimens; data not shown). Low coverage alone is less likely to bias computational scores toward zero or two. For 04SEL02 (5x coverage), where cytogenetic versus computational discrepancies occur at 2R*b* and 2R*u*, the computational karyotype is supported respectively by 81% of 208 tags and >94% of 57 tags, favoring the computational genotype by weight of evidence. The remaining six specimens with discordant inversion genotypes were sequenced to at least 10x coverage. In these cases, when the computational genotype score signaled '1' in contradiction to a homokaryotypic cytogenetic genotype (02SEL85, 02SEL006, 02SEL009, 01Osel134), the proportion of tags supporting the computational genotype ranged from 65% to >92%. For other types of genotypic disagreements between

methods, the computational score was supported by >80% of tags scored. Overall, these results suggest that computational karyotyping using tag SNPs can be successful in data derived independently of Ag1000G (Tables S5, S6), though care should be taken when this approach is applied to very low coverage samples.

Performance of tag SNPs against cytogenetically karyotyped Ag1000G specimens

We compared the cytogenetic karyotype assignments for 373 specimens in Ag1000G to their corresponding computational karyotype assignments (Table 3). Conflicts were few overall, and for every inversion, all but one conflict (involving specimen AZ0267-C, the exceptional *An. gambiae* carrier of the 2R*u* inversion) could be attributed to errors in the cytogenetically assigned scores, as genotypes imputed from both PCA and tag SNPs contradict the cytogenetic assignment. Visual reference back to the PCA plots clearly confirmed that for specimens whose cytogenetic and tag SNP assignments differed and for whom PCA karyotypes could be determined, their locations on the plot strongly agreed with the tag SNP genotype (Figure S3). Considering that we ascertained tens or hundreds of tags per specimen, and that the proportion of tags whose SNP genotype matched the computational score was greater than 83% in all except the unusual specimen AZ0267-C (Table 3), the computational scores more confidently predict the true inversion genotype than traditional cytogenetics for these five inversions. The most dramatic example is with respect to inversion 2R*u*, where we noted an unusually large number of erroneous cytogenetic genotypes of '1' (N=18/29) conflicting with both PCA and computational assignments of '0'. It is not immediately clear what could lead to such an elevated rate of cytogenetic error (which otherwise is ~4%), but it is possible

513 that the 2R*u* heterozygous loop was mistaken either for a loop created by a rare
514 inversion (sensu Pombi *et al.* 2008) in the same chromosomal region, or for a 2R*d* loop
515 in samples from regions where 2R*u* is rare (as supported by the fact all 11 cytogenetic
516 errors in *An. gambiae* were found in samples from the same small region in Cameroon,
517 six of which were scored computationally as '1' for 2R*d*).

518 Our results also highlight the pitfalls of using taxon-specific tags to genotype
519 other taxa, or populations with high levels of admixture between taxa (Table S7). As
520 expected, we find elevated numbers of cytogenetic-computational disagreements when
521 (i) 2R*c-gambiae* tags are applied to BAMAKO (60% of the 45 specimens), (ii) 2R*d-*
522 *gambiae* tags are used to genotype *An. coluzzii*, and (iii) 2R*d-gambiae* tags are applied
523 to admixed *An. gambiae-An. coluzzii* populations such as those from Guinea Bissau.
524 These disagreements involve specimens carrying inverted arrangements according to
525 cytogenetic analysis which are not tagged as inverted computationally, due to the lack
526 of correlation between tags and the inverted orientation in the heterospecific genetic
527 background.

Discussion

Analysis of the Ag1000G database allowed us to develop the first standardized computational karyotyping of the six main polymorphic chromosomal inversions in the major malaria vectors *An. coluzzii* and *An. gambiae*, despite the fact that only a small subset of specimens in the database had cytogenetic karyotype assignments (Figure 7). Direct comparison of computational karyotype scores with the cytogenetic assignment for the same specimen in Ag1000G suggests that computational karyotyping outperforms traditional cytogenetics in terms of accuracy, given that assignments are based on tens or hundreds of individual tags. Preliminary testing on specimens sequenced and computationally processed by individual laboratories outside of Ag1000G standards suggests that our tag SNPs have the potential to perform well, even on specimens sequenced to much lower depth. Our approach not only has a lower error rate compared to classical cytogenetics, but also is more widely applicable (regardless of mosquito gender, physiological status, or method of preservation), more widely accessible to those without specialized expertise, higher throughput, and therefore, ultimately cheaper to implement at scale. This method can now be used to predict inversion genotypes in previously sequenced data sets for which ecological and behavioral data may already be available. Even more important, easy large-scale adoption of this approach allows for new and properly powered association studies to be performed on ecologically and epidemiologically relevant mosquito phenotypes, studies that that would have been prohibitively ambitious when relying on cytogenetic karyotyping. In addition, this method can now facilitate sequencing experiments for which inversion karyotype is relevant at scales. Expanding the possibilities further,

551 molecular assays based on these results that will allow inversion genotyping without
552 whole genome sequencing are under development.
553 However, some important limitations exist. Computational karyotyping is strictly
554 dependent upon tag SNPs that are strongly correlated with inversion status, a
555 contingency that depends upon representative sampling. Although Ag1000G is
556 populated by samples derived from multiple countries in West, Central and East Africa,
557 *An. coluzzii* is underrepresented, as is southern Africa (Miles *et al.* 2017). Even more
558 importantly, with the exception of the cosmopolitan inversions 2L*a* and 2R*b*, the inverted
559 orientation of other rearrangements (2R*j*, 2R*c*, 2R*d*, and 2R*u*) is underrepresented in
560 the Ag1000G data that was available at the time of our analysis. It is clear that
561 population structure is an especially important factor in the application and further
562 development of tags for 2R*c* and 2R*d*. The current taxon-specific tags should not be
563 used to genotype heterospecific specimens (including BAMAKO) or samples from areas
564 where high rates of interspecific hybridization are known. The presence of strong
565 population structure means that correlations between tags and the inverted orientation
566 characteristic of the target taxon cannot be assumed in a different taxon. The absence
567 of correlation should downwardly bias the computational score, resulting in false
568 negatives when genotyping true inverted homozygotes and heterozygotes. Finally, our
569 inversion breakpoint dendrograms raise the possibility that at least one cytologically-
570 recognized inversion, 2R*c*, may have arisen repeatedly at the molecular level, a result
571 that requires further investigation beyond the scope of this study. With the exception of
572 2R*c*, 2R*d*, and 2R*j*, for which we developed taxon-specific tags, our approach implicitly
573 assumed that inversions shared by *An. gambiae* and *An. coluzzii* are monophyletic, and

574 may yield unexpected results if this assumption is violated. Accordingly, these tools
575 should be applied with caution, and there is ample room for improvement as more data
576 become available. Fortunately, our standardized approach makes it easy to
577 accommodate improvements. The success of our method thus far suggests that the
578 general approach may be suitable for studying inversions more broadly, in additional
579 malaria vectors as well as other systems where inversions are implicated in local
580 adaptation.

581 Nearly twenty years ago, Coluzzi and colleagues predicted that the then-newly-
582 assembled *An. gambiae* reference genome would facilitate our analyses of polymorphic
583 chromosomal inversions in the *An. gambiae* complex (Coluzzi *et al.* 2002). Our work
584 continues the realization of that prediction by providing, for the first time, cross-continent
585 diagnostics for multiple inversions. These computational diagnostics, and the molecular
586 diagnostics that they leverage, take us one step closer to understanding the contribution
587 of chromosomal inversions to the deadly facility of *An. gambiae* and *An. coluzzii* for
588 vectoring malaria.
589

590 **Acknowledgements**

591 We thank the Notre Dame Center for Research Computing for technical support, and C.
592 Liu, C. Sweet, and J. Young for helpful discussions. We thank M. Kern and R.
593 Montanez-Gonzalez for assistance with DNA extraction. This work was supported by
594 the National Institutes of Health (R01 AI125360 awarded to NJB). During this work,
595 NJB was supported by Target Malaria, which receives core funding from the Bill &
596 Melinda Gates Foundation and from the Open Philanthropy Project Fund, an advised
597 fund of Silicon Valley Community Foundation.

598

599

600

Figure Legends

Figure 1. Diagrammatic representation of the common polymorphic inversions (labeled brackets) on chromosome 2 in *An. gambiae*. Polytene chromosome map modified from Figure 1 and poster in Coluzzi *et al*. (2002). CT, centromere.

Figure 2. Assessment of correspondence between SNP and inversion genotype in each mosquito. For each chromosomal rearrangement and mosquito, biallelic SNP genotypes inside rearrangement boundaries were converted to a number representing the count of alternative alleles (relative to the AgamP4 reference). We applied PCA to the resulting matrix to assign each individual mosquito an inversion genotype. The expectation is that the PCA-based genotype, expressed as the number of inverted chromosomes at the focal rearrangement, should match the number of alternative alleles at SNPs predictive of inversion status (tag SNPs).

Figure 3. Overview of experimental design. For each inversion, the appropriate Ag1000G sample of mosquitoes that had been successfully karyotyped by PCA was partitioned into a training set (75%) and a validation set (25%). Ten bootstrap replicates of the training set were created from a random sample of 75% of the full training set. For each bootstrap replicate and each mosquito, higher frequency biallelic SNPs within inversion breakpoints were interrogated for genotypic concordance with the PCA-based genotype. Results were summarized across the ten replicates to create a set of candidate tag SNPs with concordance rates exceeding 80%. Candidate tags were used

624 to genotype the held-out validation set, and the computational karyotype score
625 computed across tags was compared to the PCA-based karyotype. Candidate tags
626 were also used to interrogate mosquitoes sequenced independently of Ag1000G, and
627 the computational karyotype score was compared to the associated cytogenetically
628 determined karyotype.
629
630 **Figure 4.** Neighbor-joining dendrograms reconstructed from 1,347 *An. gambiae* and *An.*
631 *coluzzii* mosquitoes from Ag1000G, using biallelic SNPs within 5 kb of inversion
632 breakpoints (15 kb for 2R*d*) having a minimum minor allele frequency of 0.01. Columns
633 represent the same inversion dendrogram, alternately color-coded by inversion
634 genotype as determined from PCA (first row), taxon (second row), or geographic source
635 (third row). Some specimens that could not be karyotyped by PCA for inversions 2R*c*,
636 2R*d*, 2R*j*, and 2R*u* had cytogenetically determined karyotypes, which were used in
637 place of PCA for color-coding the inversion genotype. 'None' refers to mosquitoes that
638 were not assigned an inversion genotype either by PCA or cytogenetically; 'Other' refers
639 to mosquitoes that were not identified taxonomically.
640
641 **Figure 5.** Histograms of computational karyotyping scores calculated by interrogating
642 tag SNPs in *An. gambiae* and *An. coluzzii* mosquitoes from the Ag1000G validation
643 sets. Note that these mean scores cluster around 0, 1, and 2.
644
645 **Figure 6.** Histograms of computational karyotyping scores calculated by interrogating
646 tag SNPs in *An. gambiae* and *An. coluzzii* mosquitoes re-sequenced independently of

the Ag1000G pipeline, often at lower sequencing depth. Scores cluster near 0, 1, and 2 with little dispersion except when taxon-specific tag SNPs are applied to a different taxon (indicated by an asterisk).

Figure 7. Map of the study area with the frequency of *An. gambiae* and *An. coluzzii* inversion genotypes inferred for up to six polymorphic chromosome 2 inversions summarized by country (and the island of Mayotte; see Table S2). Blue connecting lines point to *An. coluzzii* samples, while white connecting lines point to *An. gambiae* and hybrid/outlier populations. Image: Visible Earth, NASA. Produced with cartopy v.0.17.1.

Literature Cited

Andolfatto, P., F. Depaulis, and A. Navarro, 2001 Inversion polymorphisms and nucleotide variability in *Drosophila*. *Genet. Res.* 77: 1-8.

Ayala, D., P. Acevedo, M. Pombi, I. Dia, D. Boccolini *et al.*, 2017 Chromosome inversions and ecological plasticity in the main African malaria mosquitoes. *Evolution* 71: 686-701.

Ayala, D., A. Ullastres, and J. Gonzalez, 2014 Adaptation through chromosomal inversions in Anopheles. *Front Genet* 5: 129.

Ayala, D., S. Zhang, M. Chateau, C. Fouet, I. Morlais *et al.*, 2018 Association mapping desiccation resistance within chromosomal inversions in the African malaria vector Anopheles gambiae. *Mol. Ecol.*

Bryan, J. H., M. A. Di Deco, V. Petrarca, and M. Coluzzi, 1982 Inversion polymorphism and incipient speciation in *Anopheles gambiae s. str.* in The Gambia, West Africa. *Genetica* 59: 167-176.

Caputo, B., D. Nwakanma, F. P. Caputo, M. Jawara, E. C. Oriero *et al.*, 2014 Prominent intra-specific genetic divergence within *Anopheles gambiae* sibling species triggered by habitat discontinuities across a riverine landscape. *Mol. Ecol.* 23: 4574-4589.

Caputo, B., D. Nwakanma, M. Jawara, M. Adiamoh, I. Dia *et al.*, 2008 *Anopheles gambiae* complex along The Gambia river, with particular reference to the molecular forms of *An. gambiae s.s*. *Malar. J.* 7: 182.

Caputo, B., F. Santolamazza, J. L. Vicente, D. C. Nwakanma, M. Jawara *et al.*, 2011 The "far-west" of *Anopheles gambiae* molecular forms. *PLoS One* 6: e16415.

Cassone, B. J., M. J. Molloy, C. Cheng, J. C. Tan, M. W. Hahn *et al.*, 2011 Divergent transcriptional response to thermal stress by *Anopheles gambiae* larvae carrying alternative arrangements of inversion 2La. *Mol. Ecol.* 20: 2567-2580.

Cheng, C., J. C. Tan, M. W. Hahn, and N. J. Besansky, 2018 A systems genetic analysis of inversion polymorphisms in the malaria mosquito *Anopheles gambiae*. *Proc. Natl. Acad. Sci. U. S. A.* 115: E7005-E7014.

Cheng, C., B. J. White, C. Kamdem, K. Mockaitis, C. Costantini *et al.*, 2012 Ecological genomics of *Anopheles gambiae* along a latitudinal cline: a population-resequencing approach. *Genetics* 190: 1417-1432.

Coetzee, M., R. H. Hunt, R. Wilkerson, A. della Torre, M. B. Coulibaly *et al.*, 2013 *Anopheles coluzzii* and *Anopheles amharicus*, new members of the *Anopheles gambiae* complex. *Zootaxa* 3619: 246–274.

Coluzzi, M., 1968 Cromosomi politenici delle cellule nutrici ovariche nel complesso gambiae del genere *Anopheles*. *Parassitologia* 10: 179-183.

Coluzzi, M., V. Petrarca, and M. A. DiDeco, 1985 Chromosomal inversion intergradation and incipient speciation in *Anopheles gambiae*. *Bollettino di Zoologia* 52: 45-63.

Coluzzi, M., A. Sabatini, A. della Torre, M. A. Di Deco, and V. Petrarca, 2002 A polytene chromosome analysis of the *Anopheles gambiae* species complex. *Science* 298: 1415-1418.

Coluzzi, M., A. Sabatini, V. Petrarca, and M. A. Di Deco, 1979 Chromosomal differentiation and adaptation to human environments in the *Anopheles gambiae* complex. *Trans. R. Soc. Trop. Med. Hyg.* 73: 483-497.

Corbett-Detig, R., I. Said, M. Calzetta, M. Genetti, J. McBroome *et al.*, 2019 Fine-mapping complex inversion breakpoints and investigating somatic pairing in the *Anopheles*

gambiae species complex using proximity-ligation sequencing. *BioRxiv doi: https://doi.org/10.1101/662114*.

Costantini, C., D. Ayala, W. M. Guelbeogo, M. Pombi, C. Y. Some *et al.*, 2009 Living at the edge: biogeographic patterns of habitat segregation conform to speciation by niche expansion in *Anopheles gambiae*. *BMC Ecol.* 9: 16.

Coulibaly, M. B., N. F. Lobo, M. C. Fitzpatrick, M. Kern, O. Grushko *et al.*, 2007a Segmental duplication implicated in the genesis of inversion 2Rj of *Anopheles gambiae*. *PLoS One* 2: e849.

Coulibaly, M. B., M. Pombi, B. Caputo, D. Nwakanma, M. Jawara *et al.*, 2007b PCR-based karyotyping of *Anopheles gambiae* inversion 2Rj identifies the BAMAKO chromosomal form. *Malar. J.* 6: 133.

Dabire, K. R., S. Sawadodgo, A. Diabate, K. H. Toe, P. Kengne *et al.*, 2013 Assortative mating in mixed swarms of the mosquito *Anopheles gambiae s.s*. M and S molecular forms, in Burkina Faso, West Africa. *Med. Vet. Entomol.* 27: 298-312.

della Torre, A., 1997 Polytene chromosome preparation from anopheline mosquitoes, pp. 329-336. in *Molecular Biology of Disease Vectors: A Methods Manual*, edited by J.M. Crampton, C.B. Beard and C. Louis. Chapman & Hall, London.

della Torre, A., C. Fanello, M. Akogbeto, J. Dossou-yovo, G. Favia *et al.*, 2001 Molecular evidence of incipient speciation within *Anopheles gambiae s.s.* in West Africa. *Insect Mol. Biol.* 10: 9-18.

della Torre, A., Z. Tu, and V. Petrarca, 2005 On the distribution and genetic differentiation of *Anopheles gambiae s.s.* molecular forms. *Insect Biochem. Mol. Biol.* 35: 755-769.

Diabate, A., A. Dao, A. S. Yaro, A. Adamou, R. Gonzalez *et al.*, 2009 Spatial swarm segregation and reproductive isolation between the molecular forms of *Anopheles gambiae*. *Proc. Biol. Sci.* 276: 4215-4222.

Fontaine, M. C., J. B. Pease, A. Steele, R. M. Waterhouse, D. E. Neafsey *et al.*, 2015 Extensive introgression in a malaria vector species complex revealed by phylogenomics. *Science* 347: 1258524.

Fouet, C., E. Gray, N. J. Besansky, and C. Costantini, 2012 Adaptation to aridity in the malaria mosquito *Anopheles gambiae*: chromosomal inversion polymorphism and body size influence resistance to desiccation. *PLoS One* 7: e34841.

Fuller, Z. L., G. D. Haynes, S. Richards, and S. W. Schaeffer, 2017 Genomics of natural populations: Evolutionary forces that establish and maintain gene arrangements in *Drosophila pseudoobscura*. *Mol. Ecol.* 26: 6539-6562.

Gimonneau, G., J. Bouyer, S. Morand, N. J. Besansky, A. Diabate *et al.*, 2010 A behavioral mechanism underlying ecological divergence in the malaria mosquito *Anopheles gambiae*. *Behav. Ecol.* 21: 1087-1092.

Gimonneau, G., M. Pombi, M. Choisy, S. Morand, R. K. Dabire *et al.*, 2012a Larval habitat segregation between the molecular forms of the mosquito, *Anopheles gambiae* in a rice field area of Burkina Faso, West Africa. *Med. Vet. Entomol.* 26: 9-17.

Gimonneau, G., M. Pombi, R. K. Dabire, A. Diabate, S. Morand *et al.*, 2012b Behavioural responses of Anopheles gambiae sensu stricto M and S molecular form larvae to an aquatic predator in Burkina Faso. *Parasit Vectors* 5: 65.

Giraldo-Calderon, G. I., S. J. Emrich, R. M. MacCallum, G. Maslen, E. Dialynas *et al.*, 2015 VectorBase: an updated bioinformatics resource for invertebrate vectors and other organisms related with human diseases. *Nucleic Acids Res.* 43: D707-713.

Gray, E. M., K. A. Rocca, C. Costantini, and N. J. Besansky, 2009 Inversion 2La is associated with enhanced desiccation resistance in *Anopheles gambiae*. *Malar. J.* 8: 215.

Hanemaaijer, M. J., T. C. Collier, A. Chang, C. C. Shott, P. D. Houston *et al.*, 2018 The fate of genes that cross species boundaries after a major hybridization event in a natural mosquito population. *Mol. Ecol.* 27: 4978-4990.

Hoffmann, A. A., and L. H. Rieseberg, 2008 Revisiting the impact of inversions in evolution: from population genetic markers to drivers of adaptive shifts and speciation? *Annual Review of Ecology Evolution and Systematics* 39: 21-42.

Hoffmann, A. A., C. M. Sgro, and A. R. Weeks, 2004 Chromosomal inversion polymorphisms and adaptation. *Trends Ecol. Evol.* 19: 482-488.

Holt, R. A., G. M. Subramanian, A. Halpern, G. G. Sutton, R. Charlab *et al.*, 2002 The genome sequence of the malaria mosquito *Anopheles gambiae*. *Science* 298: 129-149.

Houle, D., and E. J. Marquez, 2015 Linkage disequilibrium and inversion-typing of the *Drosophila melanogaster* genome reference panel. *G3 (Bethesda)* 5: 1695-1701.

Jones, F. C., M. G. Grabherr, Y. F. Chan, P. Russell, E. Mauceli *et al.*, 2012 The genomic basis of adaptive evolution in threespine sticklebacks. *Nature* 484: 55-61.

Joron, M., L. Frezal, R. T. Jones, N. L. Chamberlain, S. F. Lee *et al.*, 2011 Chromosomal rearrangements maintain a polymorphic supergene controlling butterfly mimicry. *Nature* 477: 203-206.

Kapun, M., D. K. Fabian, J. Goudet, and T. Flatt, 2016 Genomic evidence for adaptive inversion clines in *Drosophila melanogaster*. *Mol. Biol. Evol.* 33: 1317-1336.

Kirkpatrick, M., 2010 How and why chromosome inversions evolve. *PLoS Biol.* 8: e1000501.

Kirkpatrick, M., and B. Barrett, 2015 Chromosome inversions, adaptive cassettes and the evolution of species' ranges. *Mol. Ecol.* 24: 2046-2055.

Kirkpatrick, M., and N. Barton, 2006 Chromosome inversions, local adaptation and speciation. *Genetics* 173: 419-434.

Lemoine, F., J. B. Domelevo Entfellner, E. Wilkinson, D. Correia, M. Davila Felipe *et al.*, 2018 Renewing Felsenstein's phylogenetic bootstrap in the era of big data. *Nature* 556: 452-456.

Lobo, N. F., D. M. Sangare, A. A. Regier, K. R. Reidenbach, D. A. Bretz *et al.*, 2010 Breakpoint structure of the Anopheles gambiae 2Rb chromosomal inversion. *Malar. J.* 9: 293.

Love, R. R., A. M. Steele, M. B. Coulibaly, S. F. Traore, S. J. Emrich *et al.*, 2016 Chromosomal inversions and ecotypic differentiation in Anopheles gambiae: the perspective from whole-genome sequencing. *Mol. Ecol.* 25: 5889-5906.

Lowry, D. B., and J. H. Willis, 2010 A widespread chromosomal inversion polymorphism contributes to a major life-history transition, local adaptation, and reproductive isolation. *PLoS Biol.* 8: e1000500.

Ma, J., and C. I. Amos, 2012 Investigation of inversion polymorphisms in the human genome using principal components analysis. *PLoS One* 7: e40224.

Main, B. J., Y. Lee, T. C. Collier, L. C. Norris, K. Brisco *et al.*, 2015 Complex genome evolution in Anopheles coluzzii associated with increased insecticide usage in Mali. *Mol. Ecol.* 24: 5145-5157.

Manoukis, N. C., J. R. Powell, M. B. Touré, A. Sacko, F. E. Edillo *et al.*, 2008 A test of the chromosomal theory of ecotypic speciation in *Anopheles gambiae*. *Proceedings of the National Academy of Science U S A* 105: 2940-2945.

795 Marsden, C., Y. Lee, C. Neimen, M. Sanford, J. Dinis *et al.*, 2011 Asymmetric introgression
796 between the M and S molecular forms of the malaria vector, *Anopheles gambiae*,
797 maintains divergence despite extensive hybridisation. *Mol. Ecol.* 20: 4983-4994.
798 Miles, A., and N. J. Harding, 2017 scikit-allel: A Python package for exploring and analysing
799 genetic variation data. http://github.com/cggh/scikit-allel. 10.5281/zenodo.597309.
800 Miles, A., N. J. Harding, G. Bottà, C. S. Clarkson, T. Antão *et al.*, 2017 Genetic diversity of the
801 African malaria vector *Anopheles gambiae*. *Nature* 552: 96-100.
802 Navarro, A., E. Betran, A. Barbadilla, and A. Ruiz, 1997 Recombination and gene flux caused by
803 gene conversion and crossing over in inversion heterokaryotypes. *Genetics* 146: 695-709.
804 Nwakanma, D. C., D. E. Neafsey, M. Jawara, M. Adiamoh, E. Lund *et al.*, 2013 Breakdown in
805 the process of incipient speciation in Anopheles gambiae. *Genetics* 193: 1221-1231.
806 Oliveira, E., P. Salgueiro, K. Palsson, J. L. Vicente, A. P. Arez *et al.*, 2008 High levels of
807 hybridization between molecular forms of *Anopheles gambiae* from Guinea Bissau. *J.*
808 *Med. Entomol.* 45: 1057-1063.
809 Pedregosa, F., G. Varoquaux, A. Gramfort, V. Michel, B. Thirion *et al.*, 2011 Scikit-learn:
810 Machine Learning in Python. *Journal of Machine Learning Research* 12: 2825−2830.
811 Petrarca, V., and J. C. Beier, 1992 Intraspecific chromosomal polymorphism in the *Anopheles*
812 *gambiae* complex as a factor affecting malaria transmission in the Kisumu area of Kenya.
813 *Am. J. Trop. Med. Hyg.* 46: 229-237.
814 Petrarca, V., G. Sabatinelli, M. A. Di Deco, and M. Papakay, 1990 The *Anopheles gambiae*
815 complex in the Federal Islamic Republic of Comoros (Indian Ocean): some cytogenetic
816 and biometric data. *Parassitologia* 32: 371-380.
817 Pombi, M., B. Caputo, F. Simard, M. A. Di Deco, M. Coluzzi *et al.*, 2008 Chromosomal
818 plasticity and evolutionary potential in the malaria vector *Anopheles gambiae sensu*
819 *stricto*: insights from three decades of rare paracentric inversions. *BMC Evol. Biol.* 8:
820 309.
821 R Core Team, 2018 R: A language and environment for statistical computing, R Foundation for
822 Statistical Computing, Vienna, Austria. https://www.R-project.org/.
823 Riehle, M. M., T. Bukhari, A. Gneme, W. M. Guelbeogo, B. Coulibaly *et al.*, 2017 The
824 *Anopheles gambiae* 2La chromosome inversion is associated with susceptibility to
825 *Plasmodium falciparum* in Africa. *Elife* 6.
826 Rishikesh, N., M. A. Di Deco, V. Petrarca, and M. Coluzzi, 1985 Seasonal variations in indoor
827 resting *Anopheles gambiae* and *Anopheles arabiensis* in Kaduna, Nigeria. *Acta Trop.* 42:
828 165-170.
829 Rocca, K. A., E. M. Gray, C. Costantini, and N. J. Besansky, 2009 2La chromosomal inversion
830 enhances thermal tolerance of *Anopheles gambiae* larvae. *Malar. J.* 8: 147.
831 Sangare, D. M., 2007 Breakpoint analysis of the *Anopheles gambiae s.s.* chromosome 2Rb, 2Rc,
832 and 2Ru inversions in *PhD Thesis, Graduate Program in Biological Sciences, University*
833 *of Notre Dame*. University of Notre Dame, Notre Dame, IN.
834 Schaeffer, S. W., 2008 Selection in heterogeneous environments maintains the gene arrangement
835 polymorphism of *Drosophila pseudoobscura*. *Evolution* 62: 3082-3099.
836 Seich Al Basatena, N. K., C. J. Hoggart, L. J. Coin, and P. F. O'Reilly, 2013 The effect of
837 genomic inversions on estimation of population genetic parameters from SNP data.
838 *Genetics* 193: 243-253.

839 Simard, F., D. Ayala, G. C. Kamdem, J. Etouna, K. Ose *et al.*, 2009 Ecological niche partitioning
840 between the M and S molecular forms of *Anopheles gambiae* in Cameroon: the
841 ecological side of speciation. *BMC Ecol.* 9: 17.
842 Tene Fossog, B., D. Ayala, P. Acevedo, P. Kengne, I. Ngomo Abeso Mebuy *et al.*, 2015 Habitat
843 segregation and ecological character displacement in cryptic African malaria mosquitoes.
844 *Evol Appl* 8: 326-345.
845 Toure, Y. T., V. Petrarca, S. F. Traore, A. Coulibaly, H. M. Maiga *et al.*, 1998 The distribution
846 and inversion polymorphism of chromosomally recognized taxa of the *Anopheles*
847 *gambiae* complex in Mali, West Africa. *Parassitologia* 40: 477-511.
848 Twyford, A. D., and J. Friedman, 2015 Adaptive divergence in the monkey flower Mimulus
849 guttatus is maintained by a chromosomal inversion. *Evolution* 69: 1476-1486.
850 Weetman, D., C. S. Wilding, K. Steen, J. Pinto, and M. J. Donnelly, 2012 Gene flow-dependent
851 genomic divergence between *Anopheles gambiae* M and S forms. *Mol. Biol. Evol.* 29:
852 279-291.
853 Wellenreuther, M., and L. Bernatchez, 2018 Eco-Evolutionary Genomics of Chromosomal
854 Inversions. *Trends Ecol. Evol.* 33: 427-440.
855 Wellenreuther, M., H. Rosenquist, P. Jaksons, and K. W. Larson, 2017 Local adaptation along an
856 environmental cline in a species with an inversion polymorphism. *J. Evol. Biol.* 30: 1068-
857 1077.
858 White, B. J., F. H. Collins, and N. J. Besansky, 2011 Evolution of *Anopheles gambiae* in relation
859 to humans and malaria. *Annual Review of Ecology Evolution and Systematics* 42: 111-
860 132.
861 White, B. J., F. Santolamazza, L. Kamau, M. Pombi, O. Grushko *et al.*, 2007 Molecular
862 karyotyping of the 2La inversion in *Anopheles gambiae*. *Am. J. Trop. Med. Hyg.* 76: 334-
863 339.
864 World Health Organisation, 2018 *World Malaria Report: 2018*,
865 https://www.who.int/malaria/publications/world-malaria-report-2018/report/en/.
866

867

868 Figure 1.

869

870

871

872 Figure 2.

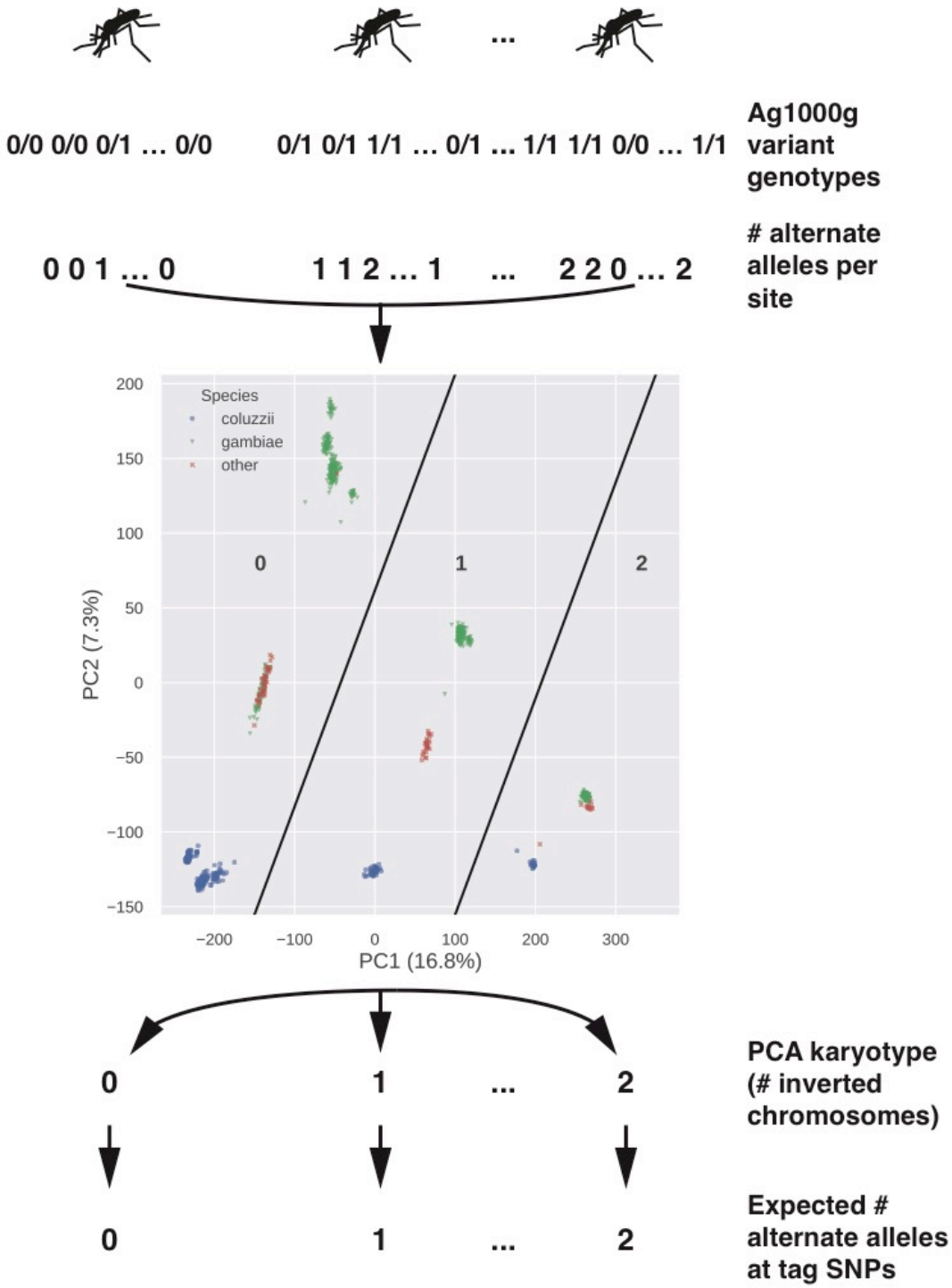

873

874

875 Figure 3.

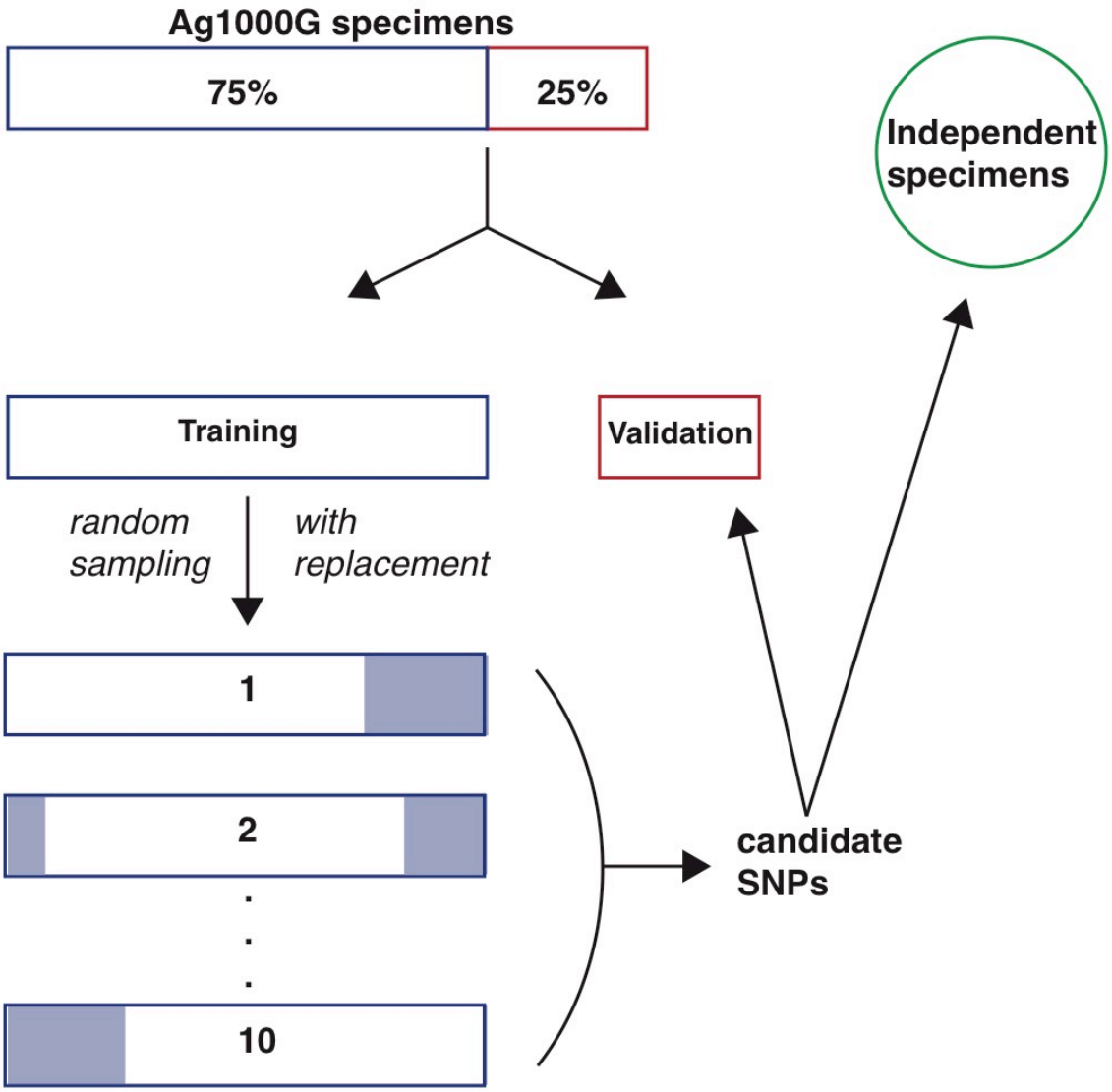

876

877 Figure 4.

878

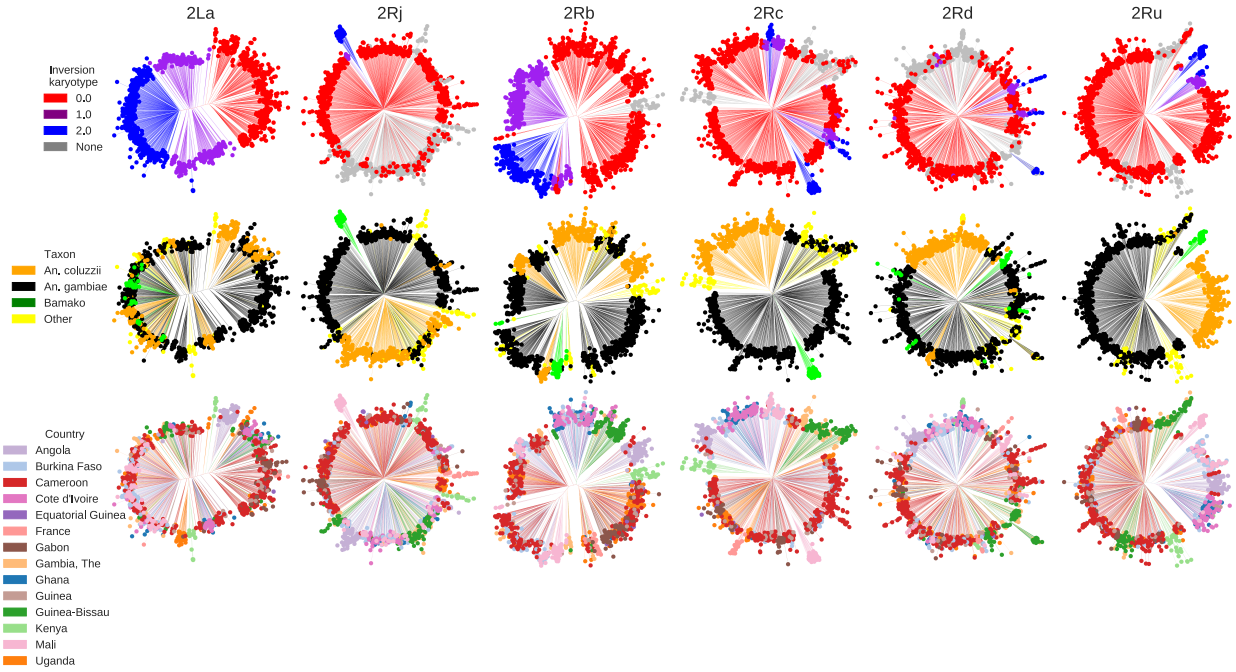

879

880

881 Figure 5.

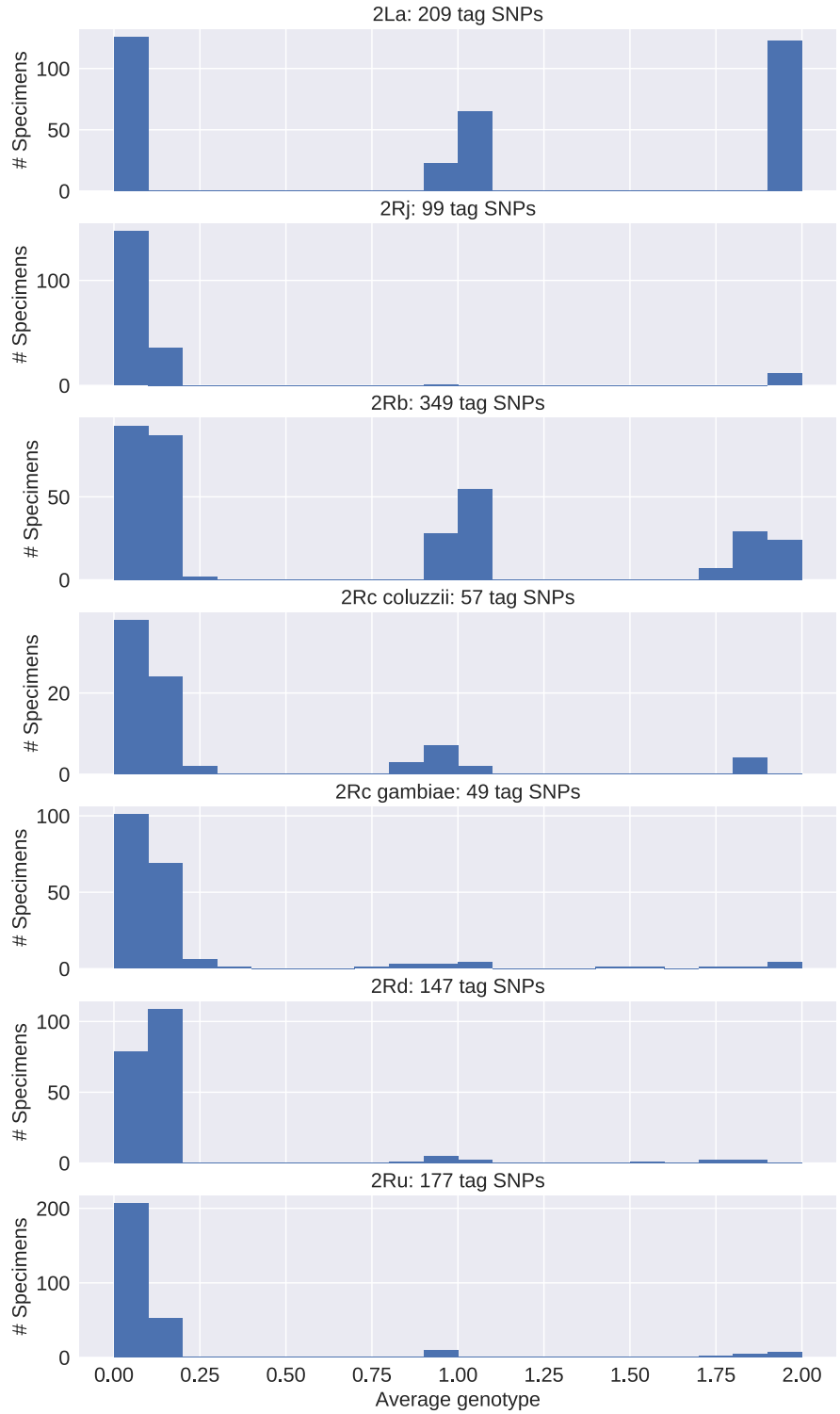

882

883

884 Figure 6.

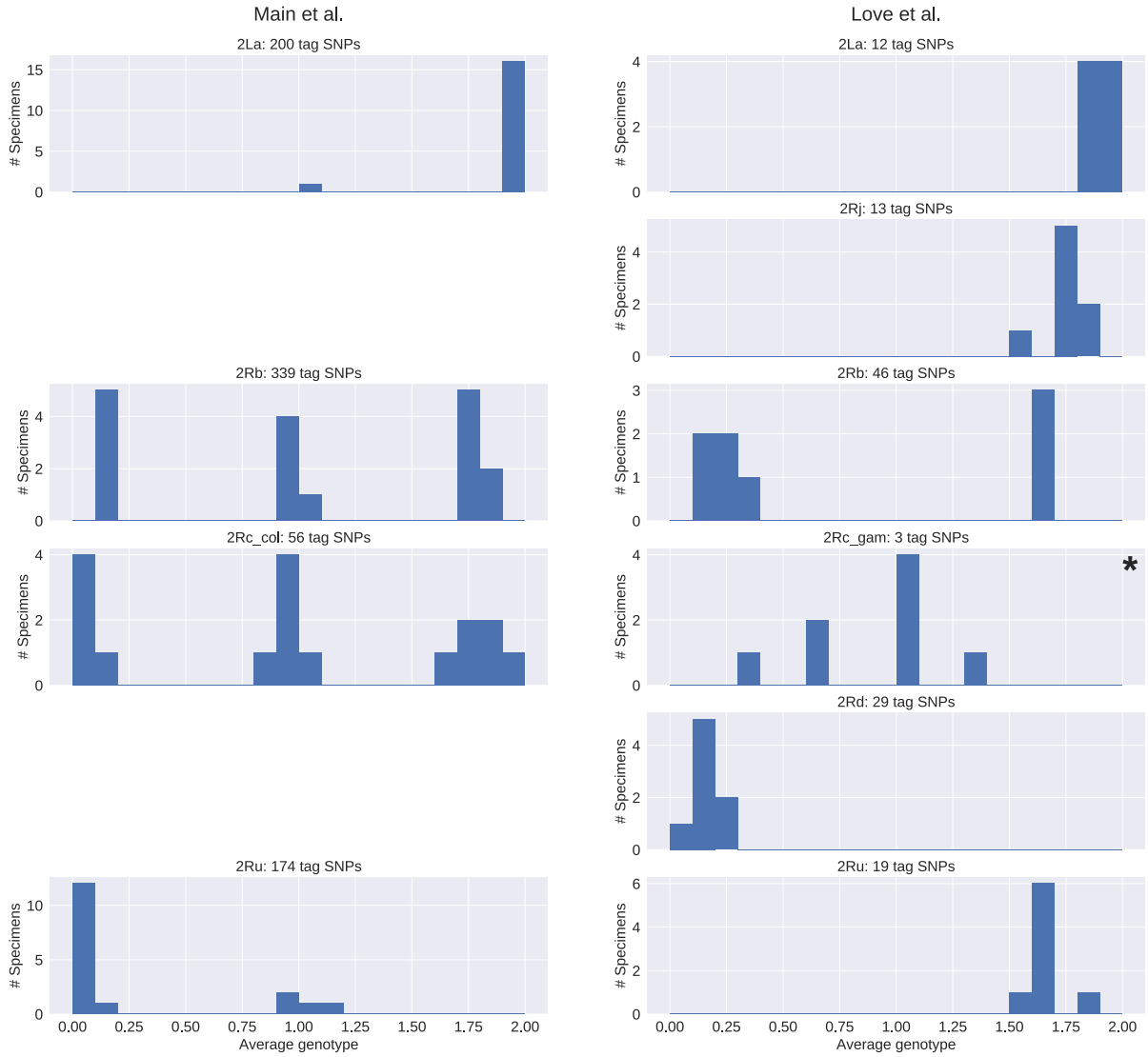

885

886

887 Figure 7.

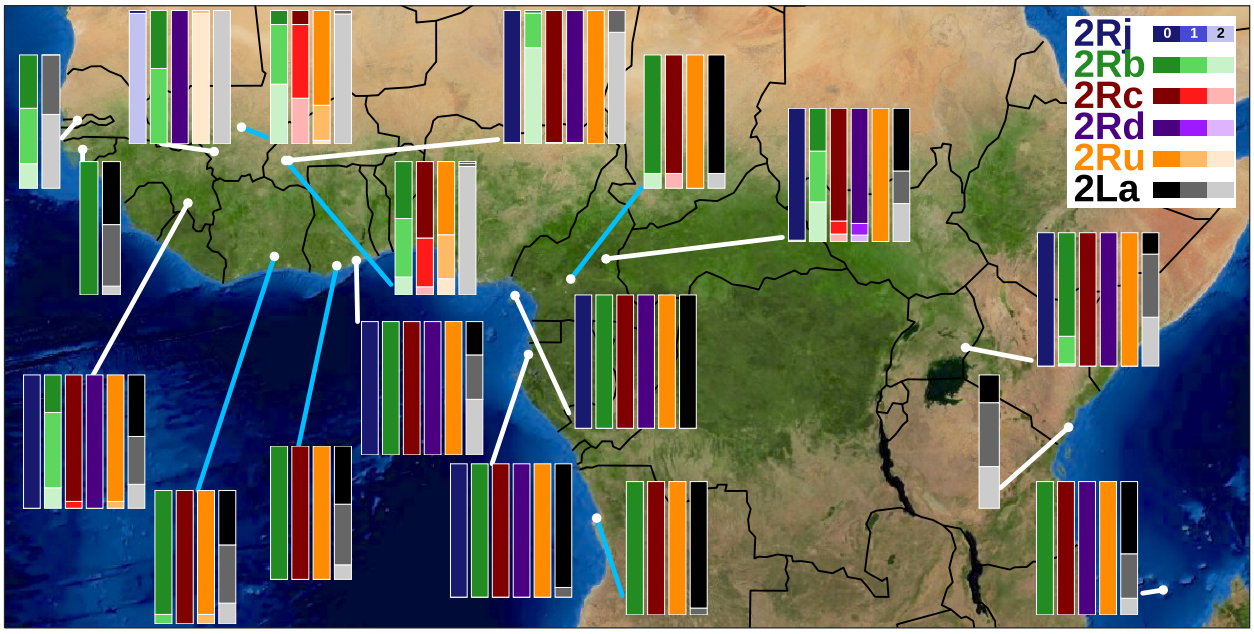

888

889

890 **Table 1.** Candidate tag SNPs predictive of inversion genotype in Ag1000G data

Inversion	Concordance Threshold	No. Tags
2L*a*	>0.995	209
2R*j-gambiae*	>0.8	99
2R*b*	>0.8	349
2R*u*	>0.8	177
2R*d-gambiae*	>0.8	147
2R*c*	>0.8	2
2R*c-coluzzii*	>0.8	57
2R*c-gambiae*	>0.8	49

891

892

893 **Table 2.** Mismatches between PCA and computational karyotypes in the Ag1000G validation sets

			Matching karyotypes		Mismatched karyotypes	
Inversion	**Total specimens**	**No. tags scored**	**No. specimens**	**% tags supporting score**	**No. Specimens**	**% tags supporting score**
2L*a*	337	168-203	337	93.6-100	0	--
2R*j-gambiae*	195	94-99	195	83.8-100	0	--
2R*b*	325	304-349	325	77.5-97.7	0	--
2R*c-coluzzii*	80	55-57	80	78.9-100	0	--
2R*c-gambiae*	196	45-49	195	59.6-100	1	67.3
2R*d-gambiae*	201	128-147	201	55.2[1]-95.9	0	--
2R*u*	286	124-177	286	76.6-100	0	--

894 [1]Next highest value is 70.1%.
895

Table 3. Discrepancies between cytogenetic and computational karyotypes in Ag1000G mosquitoes analyzed.

				Specimens with discrepancies		
Inversion Tags	**Partition**	**CYT**	**Specimens (N)**	**Mismatch CYT-TAG (%)**	**Match TAG-PCA (%)**	**No. tag SNPs scored (% matching TAG)**
2L*a*		0	117	5 (4.3)	5 (100)	200-203 (99.5-100)
		1	68	5 (7.4)	5 (100)	193-203 (100)
		2	160	2 (1.3)	2 (100)	201-203 (99.5-100)
2R*j-gambiae*	*gambiae*	0	236	0 (0)	--	–
		1	4	0 (0)	--	–
		2	45	0 (0)	--	–
2R*b*		0	127	2 (1.6)	2 (100)	348 (85.3-87.6)
		1	124	4 (3.2)	4 (100)	346-349 (86.8-93.7)
		2	121	6 (5.0)	6 (100)	331-348 (88.8-91.6)
2R*c-gambiae*	*gambiae*[1]	0	184	7 (3.8)	7 (100)	48-49 (83.7-98.0)
		1	32	3 (9.4)	2 (66.7)	47-49 (42.9[2]-91.5)
		2	24	2 (8.3)	2 (100)	48-49 (90.0-91.8)
2R*c-coluzzi*	*coluzzii*	0	13	1 (7.7)	1 (100)	56 (87.5)
		1	25	0 (0)	--	–
		2	16	0 (0)	--	–
2R*d-gambiae*	*gambiae*	0	234	9 (3.8)	9 (100)	143-147 (84.9-96.6)
		1	28	4 (14.3)	4 (100)	146-147 (88.4-93.9)
		2	22	3 (13.6)	3 (100)	146-147 (89.1-91.8)
2R*u*	*col+gam*	0	263	1 (0.38)	1 (100)	176 (85.2)
		1	29	18 (62.1)	18 (100)	170-177 (88.7-99.4)
		2	47	1 (2.1)	1 (100)	176 (97.2)

CYT, cytogenetic genotype; TAG, computational genotype; PCA, genotype inferred by PCA.

[1]*An. gambiae* excluding BAMAKO

[2]This value corresponds to one of three non-BAMAKO *An. gambiae* carriers of the 2R*u* inversion, AZ0267-C. The next highest value is 85.7.